Physical conditions of single-longitudinal-mode operation for high-power all-solid-state lasers

Huadong Lu, Jing Su, Yaohui Zheng,* and Kunchi Peng

State Key Laboratory of Quantum Optics and Quantum Optics Devices, Institute of Opto-Electronics, Shanxi University, Taiyuan, Shanxi 030006, China

**Corresponding author:yhzheng@sxu.edu.cn*

Received October 14, 2013; revised December 20, 2013; accepted January 5, 2014; posted January 15, 2014 (Doc. ID 199369); published February 18, 2014

The optimal physical conditions of single-longitudinal-mode (SLM) operation for continuous-wave all-solid-state lasers with high output powers are investigated theoretically and experimentally. The dependence of the operation conditions on the linear and nonlinear intracavity losses of the laser is numerically calculated. The theoretical analysis is demonstrated by the experimental measurements on a home-made Nd:YVO_4 laser. The stable SLM output up to 33.7 W with optical–optical conversion efficiency of 44.9% at 1064 nm wavelength is recorded for over 7 h. The experimental results are in good agreement with the theoretical expectation. © 2014 Optical Society of America

OCIS codes: (140.3600) Lasers, tunable; (140.3515) Lasers, frequency doubled; (140.3560) Lasers, ring; (140.3570) Lasers, single-mode.

http://dx.doi.org/10.1364/OL.39.001117

All-solid-state continuous-wave (CW) single-longitudinal-mode (SLM) lasers have been extensively utilized in a variety of scientific research and technology applications. Especially, CW Nd:YVO_4 lasers with SLM 1064 nm output are important pump sources of optical parametric oscillators used for extending the wavelength of a laser [1] or generating squeezed and entangled states of light [2]. They are also applied in advanced experimental investigation, such as atomic trapping [3], gravitation-wave detection [4], and quantum information. To satisfy the requirements of various applications, long-stable SLM lasers with high output power and perfect beam quality are desired. It is more difficult to keep a high-power laser stably operating due to the influences of larger thermal effect in the gain medium and mode competition inside the laser resonator. A lot of technical improvements, such as optimizing the mode size [5], choosing specially designed composite [6] or lower-doped [7] laser mediums, and using dual-end-pumped and directly pumped schemes [8], have been exploited to reduce the thermal effect in the gain medium, and thus perfect single-transverse-mode operating has been realized in CW laser systems. Besides the transverse-mode quality, the longitudinal-mode characteristic of a laser is also crucial for many precise experiments and metrology. A most effective method for suppressing multi-longitudinal-mode (MLM) oscillating and mode-hopping in solid-state resonators is the intracavity second-harmonic generation (SHG). The SHG process increases the nonlinear loss of the fundamental wave due to frequency conversion, and it has been well proved that when the nonlinear loss of the lasing mode of a SLM laser is only half of its nonlasing modes, the oscillation of nonlasing modes can be naturally suppressed [9]. Based on the principle of intracavity SHG suppression, CW all-solid-state lasers at 532 nm with low-intensity noise and stable SLM operation were demonstrated first in [10]. Successively, this concept was simply extended to suppress mode hopping in a resonator producing the fundamental frequency laser by inserting an intracavity SHG crystal [11]. In [11], a mode-hop-free tunable SLM laser with 25 W output power, linewidth of less than 2.5 MHz, and optical-to-optical conversion efficiency of better than 35% from the pump wavelengths of 808–1064 nm was successfully achieved. A commercial product of an SLM 1064 nm laser is supplied by the Innolight GmbH, the maximal output power, the frequency bandwidth, and M^2 value of which are 55 W, ~1 kHz, and ~1.3, respectively [12]. So far, although the commercial products of SLM all-solid-state lasers at 532 and 1064 nm have been available, the optimal SHG suppression conditions have not been quantitatively analyzed to the best of our knowledge. We find that there is a functional dependence between the intracavity linear loss and nonlinear loss of a laser resonator, from which the optimal operating conditions for generating stable output of a SLM fundamental wave can be obtained. In this Letter we first deduce the function relationship between the normalized linear loss and the nonlinear conversion loss in a SLM resonator with a intracavity nonlinear crystal for SHG. Then the critical condition for SLM and MLM operation of the solid-state laser resonator is analyzed, and the dependence of the output power on the transmission of the output coupler of the resonator is numerically calculated for different nonlinear losses. At last, the experimental results on a home-made all-solid-state Nd:YVO_4 laser with an intracavity LiB_3O_5 (LBO) crystal (lithium triborate) used for SHG suppression are presented. The experimental observation and the theoretical calculation are in good agreement, which provides us a feasible way to optimize the physical parameters of a high-power all-solid-state CW SLM laser. When the gain medium and the resonator configuration are fixed, we may achieve the optimal SLM operation of a laser by adjusting the temperature of the nonlinear crystal or choosing a suitable transmission of output coupler.

To obtain a stable SLM fundamental-wave laser without MLM oscillation and mode hopping, the net gain of the lasing (λ_i) and nonlasing (λ_j) modes should satisfy the following equations [13]:

$$\frac{G_i}{2g_0(\lambda_i,1)l}=\frac{1}{1+\frac{2S(\lambda_i)}{S_0(\lambda_i,1)}}-\alpha(\lambda_i)-2\varepsilon(\lambda_i,\lambda_j,\gamma)\frac{S(\lambda_i)}{S_0(\lambda_i,1)}=0, \tag{1a}$$

$$\frac{G_j}{2g_0(\lambda_j,1)l}=\frac{1}{1+\frac{2S(\lambda_i)}{S_0(\lambda_i,1)}}-\alpha(\lambda_j)-4\varepsilon(\lambda_i,\lambda_j,\gamma)\frac{S(\lambda_i)}{S_0(\lambda_i,1)}<0, \tag{1b}$$

where $\gamma=\Delta\lambda_{\mathrm{NL}}/\Delta\lambda_g$ is the ratio between the nonlinear spectral bandwidth ($\Delta\lambda_{\mathrm{NL}}$) of the nonlinear crystal and the gain bandwidth ($\Delta\lambda_g$) of the laser crystal; $G_{i,j}$ is the net gain; g_0 is the small signal gain factor; l is the length of the gain medium; $\alpha=(L+t)/2g_0l$, where L is the intracavity linear losses and t is the transmission of the output coupler; $\varepsilon=(\mathrm{KS}_0)/(4g_0l)$, where K is the factor of nonlinear conversion; S_0 is the saturation power; and S is the fundamental-wave power.

According to Eq. (1a) and inequality (1b), the criterion condition for laser operation in the SLM region is obtained:

$$\frac{1}{2}-2\mathrm{sinc}^2\left(\frac{1.39}{2\gamma}\right)<\frac{\alpha_0}{\sqrt{(\alpha_0-\varepsilon_0)^2+4\varepsilon_0}-(\alpha_0+\varepsilon_0)}, \tag{2}$$

where α_0 and ε_0 are the normalized linear and nonlinear loss, respectively. When the left side of Eq. (2) is smaller than its right side, the laser will operate at the SLM state; otherwise MLM will oscillate. The solid curve in Fig. 1 shows the dependence of ϵ_0 on α_0, which is obtained from Eq. (2) when its left side equals its right side. The physical parameters used for Fig. 1 are the gain bandwidth of Nd:YVO_4 crystal, $\Delta\lambda_g=255$ GHz; the nonlinear spectral bandwidth of LBO with the length of 18 mm, $\Delta\lambda_{\mathrm{NL}}=125.7$ GHz; and $\gamma=\Delta\lambda_{\mathrm{NL}}/\Delta\lambda_g=0.493$. In the region above the curve the left side of Eq. (2) is smaller than the right side, so the laser will be in SLM operation. Below the curve, the left side of Eq. (2) is larger than the right side, and thus the laser will operate at the MLM state. When the configuration of the resonator and the laser medium have been chosen, the parameter γ will be a fixed value. In this case, we can adjust the parameters ϵ_0 or α_0 to make the laser operate at the SLM state. Although there is a wide region for SLM operation in Fig. 1, we should also consider how to obtain a higher output power for a given laser. For a stable SLM laser with intracavity nonlinear conversion loss (ϵ), the oscillation condition is expressed as [14]

$$gl=t+L+\epsilon, \tag{3}$$

where g is the gain coefficient per unit length of laser medium, and we have

$$g=\frac{g_0}{1+\frac{S}{S_0}}. \tag{4}$$

The nonlinear conversion efficiency ϵ equals

$$\epsilon=\mathrm{KS}. \tag{5}$$

Substituting Eqs. (4) and (5) into Eq. (3), we get the output power (P) of the fundamental wave:

$$P=A\cdot t\cdot S, \tag{6}$$

where A stands for the average cross section of the laser beam in the gain medium. Figure 2 is the functions of output power versus the transmission of the output coupler of the laser for three different nonlinear conversion factors (K), in which the experimentally measured parameters for our system, $L=2.3\%$, $S_0=8.30827\times10^6$ W/m^2, $A=1.5$ mm^2, $g_0l=0.087P_{\mathrm{in}}$, and $P_{\mathrm{in}}=75$ W, are utilized. We can see there is an optimal $t=t_{\mathrm{opt}}$ for a given K, where the output power reaches to the highest point, and t_{opt} increases when K increases.

To prove the above theoretical analysis, we design and build a single-end laser diode (LD)-pumped all-solid-state laser, which is shown in Fig. 3. The pump source is a commercially available fiber-coupled diode array which produces the partially polarized laser at 888 nm. The output beam of the LD is coupled into the laser resonator and is focused at the center of the gain medium. The optical coupler is a telescope system consisting of two lenses f_1 and f_2 with the focal lengths of 30 and 80 mm, respectively. A figure-eight-shaped ring resonator is constructed by four mirrors (M_1–M_4). The input coupler M_1 is a convex mirror coated with high-reflective (HR) films for 1064 nm and antireflective (AR) films for 888 nm; the

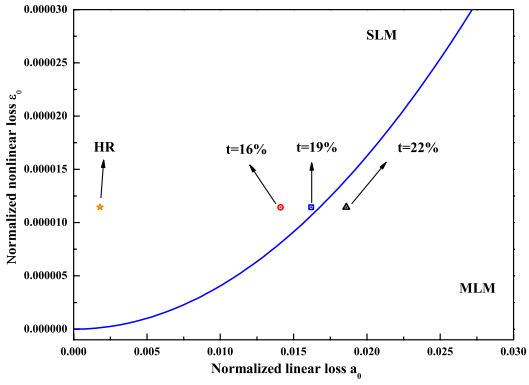

Fig. 1. Dependence of nonlinear loss ϵ_0 on linear loss α_0 for the criterion condition of SLM operation.

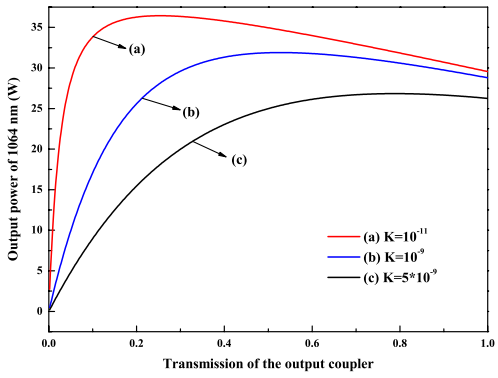

Fig. 2. Laser output power (P) as a function of the transmission (t) of the output coupler for different K.

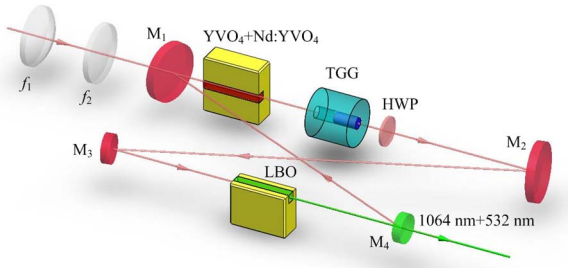

Fig. 3. Schematic of the single-end LD-pumped laser.

cavity mirror M_2 is also a convex mirror coated with HR films for 1064 nm. The curvature radius of M_1 and M_2 are both 1500 mm. The cavity mirror M_3 is a plano–concave mirror of 100 mm curvature radius coated with HR films for 1064 nm. The output coupler M_4 is also a plano-concave mirror of 100 mm radius coated with the fractional transmission at 1064 nm. The gain medium of the laser is a composite YVO_4/Nd:YVO_4 (yttrium canadate/Nd^{3+}-doped yttrium vanadate) crystal with a length of 23 mm which includes an undoped end cap 3 mm long and a 0.8% Nd-doped rod 20 mm long. For keeping constant polarization, a end facet of the laser medium is made as the wedge shape of 1.5° [15]. The Nd:YVO_4 crystal is cut along the a axis, the front end-face of which is coated with AR films for wavelengths of both 1064 and 888 nm, and the second end-face is coated with AR films only for 1064 nm. To maintain the unidirectional operation of the laser, an optical diode consisting of an 8 mm long terbium gallium garnet rod surrounded by a magnetic field and an AR-coated half-wave plate at 1064 nm is applied. The nonlinear loss is induced by a LBO nonlinear crystal with the dimensions of 3 mm× 3 mm × 18 mm. The nonlinear crystal is cut for implementing type-I noncritical phase matched SHG and is placed at the position of the beam waist of the oscillating laser between M_3 and M_4. The LBO crystal is put in a copper oven, the temperature of which is controlled at the phase-matching temperature for SHG by a homemade temperature controller with the precision of 0.1 K.

Before inserting the nonlinear LBO crystal into the resonator, the laser operates at the MLM state when the pump power is higher than 75 W. The longitudinal-mode structure of the fundamental wave through a scanned Fabry–Perot cavity (F-P-100, Yuguang Co., Ltd.) is shown in Fig. 4(a), where three longitudinal modes simultaneously oscillate. After the LBO crystal at the phase-matching temperature of 422 K is inserted into the resonator, if the output coupler coated with HR films for 1064 nm and AR films for 532 nm is utilized, the laser enters the SLM operation [Fig. 4(b)]. In this case, the output power of the fundamental wave only is 400 mW since the 532 nm SHG becomes the main output. For improving the power of the fundamental wave, we gradually increase the transmission of the output coupler at 1064 nm and find that when the transmission is less than 19%, the laser can stably operate at the SLM state. However, if the transmission is higher than 19%, MLM will start to oscillate. That is because, according to the calculated result using the above-mentioned parameters of our system, when $t > 19\%$, the operating point of the

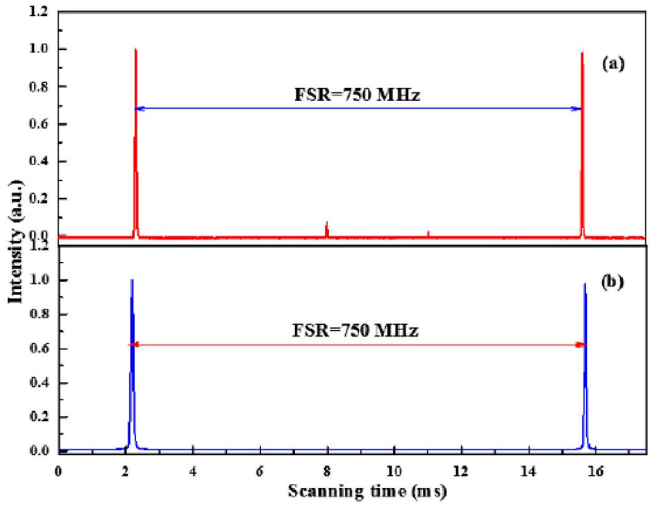

Fig. 4. Longitudinal-mode structure of the laser (a) without and (b) with the nonlinear crystal LBO ($P_p = 75$ W).

laser has entered into the region of MLM oscillation. In Fig. 1, four experimental points are marked, where the points of $t = 0$, 16%, and 19% are in the SLM region, where stable SLM operation is obtained. At the point of $t = 22\%$ the laser is in the region of MLM operation, where MLM operation is observed. The experimental results are in good agreement with the theoretical expectation.

Figure 5 shows the dependence of the output power of the fundamental wave on the temperature of the LBO crystal for the laser with the transmission of the 19% output coupler. The coefficient of the nonlinear loss (ϵ_0) in inequality (2) depends on the temperature of the nonlinear crystal [16]:

$$\epsilon_0 = \epsilon' \sin c^2\left[\frac{\left(2\lambda_f \frac{dn_z}{dT} - \lambda_s \frac{dn_y}{dT}\right)\Delta T l}{2}\right], \tag{7}$$

where $\lambda_f = 1.064$ μm and $\lambda_s = 0.532$ μm are the fundamental and second-harmonic wavelengths, respectively; $dn_z/dT = (-6.3 + 2.1\lambda_f) \times 10^{-6}$ and $dn_y/dT = -13.6 \times 10^{-6}$ are the temperature coefficient of the refractive index of the fundamental and second-harmonic wave

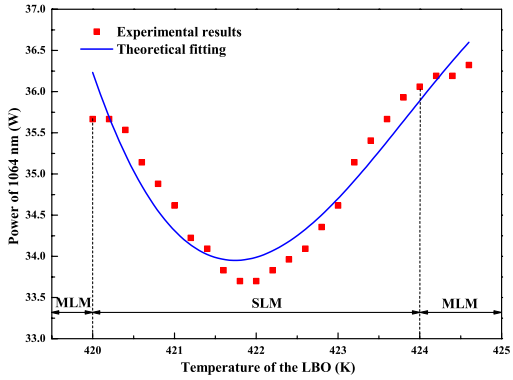

Fig. 5. Output power of 1064 nm versus the temperature of the LBO.

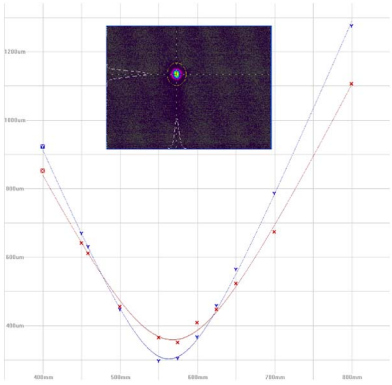

Fig. 6. Measured M^2 values and the spatial beam profile for a 1064 nm laser.

in the nonlinear crystal; ΔT is the temperature mismatching; and ϵ' is the normalized optimal nonlinear conversion loss. When the temperature of the nonlinear crystal is the optimal phase-matching temperature, that is, $\Delta T = 0$, we have $\epsilon_0 = \epsilon'$. Substituting Eq. (7) in inequality (2), we find that when the temperature of the LBO is changed ± 2 K around 422 K the laser operates at the region of SLM. Once the temperature is lower than 420 K or higher than 424 K, the laser will start MLM oscillation. Although at 420 and 424 K the highest output powers (35.67 and 36.06 W, respectively) can be achieved, the temperature points are too close to the criterion points of MLM oscillation and thus are not very stable. At the phase-matching temperature of 422 K, the laser stably operates in the region of SLM, and the output power only reduces 2.36 W less than the highest values. Under the pump power of 75 W, the stable output powers of 33.7 W at 1064 nm and 1.13 W at 532 nm are simultaneously produced by the laser with $t = 19\%$ and $T = 422$ K. The optical-to-optical efficiency from 888 to 1064 nm conversion is better than 44.9% (considering the output of 532 nm, the total efficiency is 46.5%). In order to measure the long-term power stability of the SLM laser, a power meter supplied by Coherent Inc. (LabMax-Top) is applied, which can record the trend of the power values automatically for more than 10 h with a sample per second. The measured long-term power stability is better than $\pm 0.31\%$ (peak-to-peak) for 7 h without mode hopping. The frequency bandwidth of the output SLM 1064 nm laser is 1.5 MHz, which is measured by means of a heterodyne beat signal between the 1064 nm laser and a reference laser from a low-power 1064 nm laser with a linewidth of 150 kHz [17]. The measured frequency drift is less than ± 10 MHz/ min when the laser is free running. The beam quality of the laser is measured by a M^2 meter (M^2 – 200, Spiricon Inc.), and the values of M_x^2 and M_y^2 are 1.14 and 1.13, respectively. The measured caustic curve and the corresponding spatial beam profile are shown in Fig. 6 and its inset, respectively.

In summary, we theoretically analyze the dependence of the SLM operating condition on intracavity linear and nonlinear losses in an all-solid-state laser with a nonlinear crystal inside the resonator. The experimental measurements are in good agreement with theoretical expectations. Under a certain pump power, the optimal operating condition for achieving stable SLM output of high power can be met by choosing an appropriate transmission of the output coupler inside the SLM region of Fig. 1. The presented work provides a useful reference for the design of an SLM high-power solid-state lasers.

This research was supported by the National Basic Research Program of China (No. 2010CB923101), National Major Scientific Equipment Developed Project of China (Grant No. 2011YQ030127), and National Natural Science Foundation of China (Grant No. 61227015).

References

1. E. V. Kovalchuk, D. Dekorsy, A. I. Lvovsky, C. Braxmaier, J. Mlynek, A. Peters, and S. Schiller, Opt. Lett. **26**, 1430 (2001).
2. H. Vahlbruch, M. Mehmet, S. Chelkowski, B. Hage, A. Franzen, N. Lastzka, S. Gobler, K. Danzmann, and R. Schnabel, Phys. Rev. Lett. **100**, 033602 (2008).
3. K.-K. Ni, S. Ospelkaus, D. Wang, G. Quemener, B. Neyenhuis, M. H. G. Miranda, J. L. Bohn, J. Ye, and D. S. Jin, Nature **464**, 1324 (2010).
4. B. Willke, Classical Quantum Gravity **24**, S389 (2007).
5. T. Y. Fan and R. L. Byer, IEEE J. Quantum Electron. **24**, 895 (1988).
6. D. Y. Chen, X. D. Li, Y. Zhang, X. Yu, F. Chen, R. P. Yan, Y. F. Ma, and C. Wang, Laser Phys. Lett. **8**, 46 (2011).
7. E. Cheng, D. R. Dudley, W. L. Nighan, Jr., J. D. Kafka, D. E. Spence, and D. S. Bell, "Lasers with low doped gain medium," U.S. patent 6,185,235 (February 6, 2001).
8. Q. Liu, J. Liu, Y. Jiao, J. Feng, and K. Zhang, Chin. Phys. Lett. **29**, 054205 (2012).
9. K. I. Martin, W. A. Clarkson, and D. C. Hanna, Opt. Lett. **22**, 375 (1997).
10. K. I. Martin, W. A. Clarkson, and D. C. Hanna, Opt. Lett. **21**, 875 (1996).
11. K. M. Murdoch, D. A. Clubley, and M. J. Snadden, Proc. SPIE **7193**, 71930 (2009).
12. Coherent, "Mephisto/Mephisto-S," http://www.coherent.com/Products/index.cfm?2064/Mephisto-Mephisto-S.
13. S. Greenstein and M. Rosenbluh, Opt. Commun. **248**, 241 (2005).
14. W. Koechner, *Solid State Laser Engineering* (Springer, 1999), p. 91.
15. Y. Zheng, F. Li, Y. Wang, K. Zhang, and K. Peng, Opt. Commun. **283**, 309 (2010).
16. K. Kato, IEEE J. Quantum Electron. **30**, 2950 (1994).
17. W. Wang, H. Lu, J. Su, and K. Peng, Appl. Opt. **52**, 2279 (2013).